The effective resistance of pipeline steels to running ductile factures; modelling of laboratory test data

R. M. Andrews[1], I. C. Howard[2], A. Shterenlikht[2] and J. R. Yates[2]

[1] Advantica Technology, Loughborough, UK
[2] Structural Integrity Research Institute; University of Sheffield, UK

ABSTRACT: *This paper describes a technique that uses ductile damage mechanics to cross-correlate different experimental results. The cross-correlation is achieved via FE modelling of the corresponding experiments and finding the best-fitted damage parameters. In this work FE modelling was performed in the Abaqus/Explicit code using the Gurson-Tvergaard (GT) damage model. The technique is demonstrated by extracting the shear-associated energy from the total energy, absorbed in the Charpy test. The shear-related GT parameters are tuned via FE modelling of a novel specimen aimed at simulating the running slant crack in a pipeline. The $CTOA_C$ estimated from this specimen was 8°, which is consistent with results, reported previously by others. GT parameters related to the flat fracture were tuned via FE modelling of notch tensile tests.*

INTRODUCTION

Although the limitations of the Charpy test as an indicator of crack growth resistance have long been recognised [1,2], Charpy energy will probably continue to be a toughness-related parameter for foreseeable future. Part of these limitations come from the fact that only one parameter, the total energy absorbed, is obtained from the conventional Charpy test. The appearance of the fracture surface, often rich in informative details, is usually ignored. The analysis of this surface is a key to a successful extension of applicability of the Charpy test.

Visual examination of the fracture surface of a Charpy sample after the test reveals the complex nature of the fracture process. Figure 1c shows one of the broken Charpy samples, TL-oriented, made of X80 grade API 5L pipeline steel. It is easy to observe the areas of initial flat fracture, shear lips, delaminations and the final shear region. Only the part of the total absorbed energy associated with shear fracture should be related to the slant fracture in pipelines. The techniques of ductile damage mechanics can be used as a tool for separating the Charpy energy into parts associated with shear and flat fracture, via finite element modelling.

The finite element model of the Charpy tests should therefore consist of
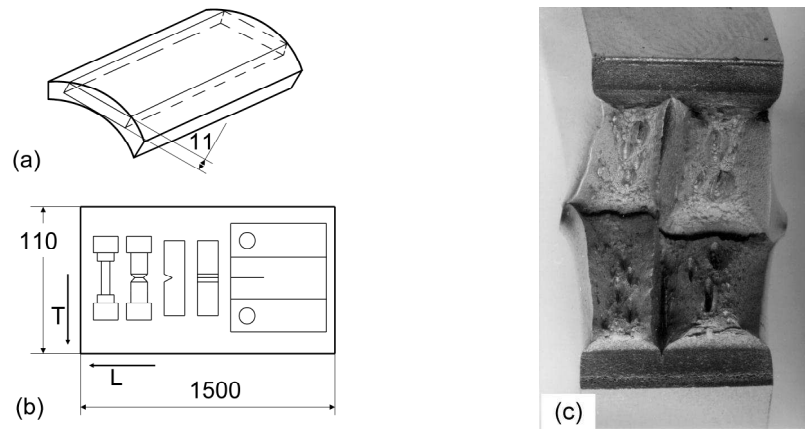
Figure 1: showing a) orientation of a plate of material cut out of a pipe, b) orientation and position of specimens machined and c) Fracture surface of a Charpy specimen machined of X80 grade API L5 pipeline showing areas of initial flat fracture, shear lips, delaminations and the region of final shear fracture.

specific groups of elements that will fracture according to one or other (shear or flat) mechanism. It is necessary to have two tuned sets of damage parameters, one for each group of elements.

Flat fracture damage parameters were tuned via finite element modelling of notch tensile tests. The specially designed shear test was used for tuning the slant fracture damage parameters.

All specimens (including the Charpy samples) were machined out of a 1219mm diameter x 13.8 mm wall X80 grade API 5L pipe, provided by Advantica Technology. The cutting scheme is shown in Figure 1a,b. The chemical analysis of this pipe was performed by Europipe [3] and is set out in Table 1. The yield and ultimate tensile stresses were found to be $S_Y = 551$ MPa and UTS = 620 MPa.

TUNING OF DUCTILE DAMAGE MODELLING PARAMETERS

The Gurson-Tvergaard [4-6] (GT) ductile damage model, as implemented in the Abaqus/Explicit finite element code, was used in this work. The damage parameters in this model are dimensionless coefficients q_1, q_2, q_3. The aim of the tuning is to find the best fitted values for GT parameters in models of appropriate experiments.

The other GT parameters required are the critical value of the void

TABLE 1: Chemical composition of provided X80 grade API 5L linepipe steel

El.	C	Si	Mn	P	S	Al	Cu	Cr	Ni	Mo	V	Nb	N	B
Wt%	0.11	0.5	2.0	0.02	0.003	0.05	0.1	0.1	0.1	0.05	0.01	0.05	0.006	0.0005

volume fraction, f_c, at which void coalescence starts and the value of void volume fraction at which the material loses stress carrying capacity, f_f. These were chosen according to [6] as $f_c = 0.15$ and $f_f = 0.25$.

Initial voidage, f_0, was obtained from the chemical composition using Franklin's [7] formula:

$$f_0 = 0.054(S\% - 0.001/Mn\%) \qquad (1)$$

Use of the values from Table 1 gives $f_0 = 0.135 \times 10^{-3}$.

Flat fracture

Previous experience has shown [8-11] that notch tensile tests are suitable for tuning of ductile damage parameters for flat fracture. The similarity of the experimental and modelling 'load - diametral contraction' curves was used as the criterion for obtaining the best-fitted values of the GT damage parameters.

Four notch tensile specimens were machined with notch radii of 2.5 mm and 6 mm, two of each. The tensile tests were performed under displacement control. Diametral contraction and load were measured during each test.

Finite element modelling of the tensile tests was performed using 2D axisymmetrical meshes, shown in Figure 2a-b. The damage cell size, L_c, was taken to be 0.25 mm by analogy with the previous work [8,9].

Figure 2c shows the best-fitted modelling `load – diametral contraction' curve together with the experimental ones for tensile specimens with notch radii equal to 6 mm. A similar level of fitting was achieved for 2.5 mm notch tensile specimens.

The GT best-fitted parameters were found to be $q_1 = 1.6$, $q_2 = 1.3$, $q_3 = 2.56$ for notch radius $r = 6$ mm, and $q_1 = 1.6$, $q_2 = 1.1$, $q_3 = 2.56$ for notch radius $r = 2.5$ mm. These values indicate that the q_2 parameter depends on triaxiality level. This unusual result is probably a consequence of using axisymmetric FE models for a highly anisotropic material as linepipe steel [12]. It was finally decided to use the average value for this parameter, $q_2 = 1.2$, as the most effective measure of this damage parameter.
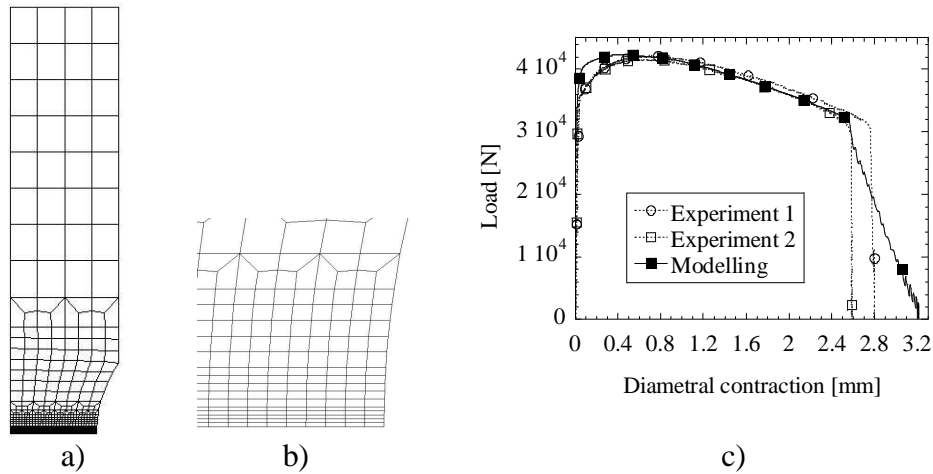
Figure 2: showing a) axisymmetric finite element mesh of a quarter of a notch tensile specimen with notch radius $r = 6$ mm, b) enlarged bottom area of the mesh, c) experimental and best-fitted modelling `load – diametrical contraction' curves for specimens with $r = 6$ mm.

Shear fracture

A new DCB-like specimen was designed. It exhibits the following properties:

- It is cut directly from a pipe, without any subsequent flattening;
- High constraint in the test section was achieved by means of two thicker loading arms;
- It has the maximum possible width, thickness and ligament, which makes the stress-strain conditions at the crack tip and ahead (size of the plastic zone) close to that of a pipeline;
- It has a flat surface near the crack tip for ease of CTOA measurement.

Similar specimen geometries reported in literature [13-16] do not satisfy all of the above conditions.

Specimens with three ligament thicknesses, 4mm, 8mm and 10mm, were machined, three of each. Sufficient constraint in 4mm thick ligament specimens was provided by 11mm thick arms. However 8mm and 10mm thick specimens had to be clamped through additional holes to substantial loading plates in order to achieve the desired constraint level. This design can be seen in Figures 3e and 4b.

CTOA was chosen as the appropriate fracture propagation characterising parameter. The similarity between the measured value of the critical CTOA, $CTOA_C$, and that obtained through FE modelling was used as a criterion for
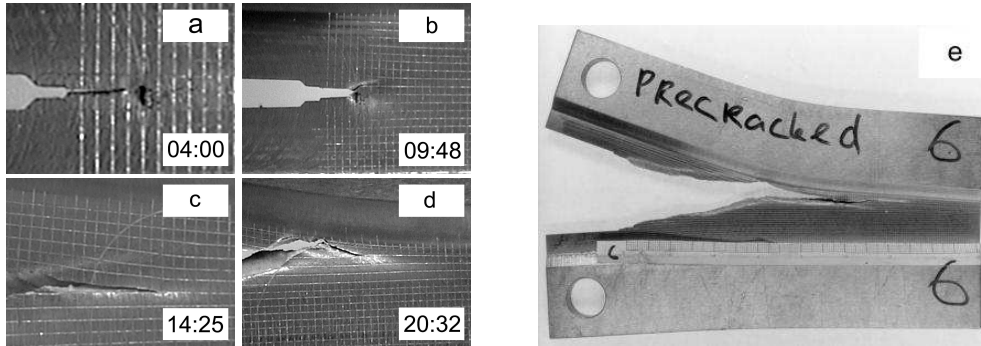
Figure 3: showing a)-d) four captured frames showing crack propagation in 4mm thick ligament specimen No. 6. Time from the start of the test is shown in the right bottom corner in format `minutes:seconds'; e) 4mm thick shear specimen after the test.
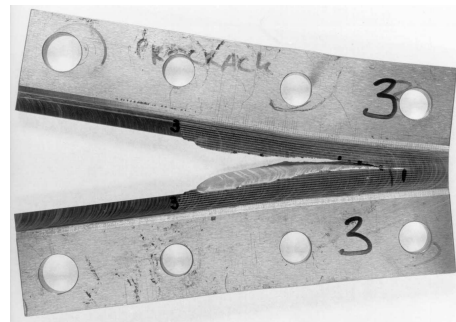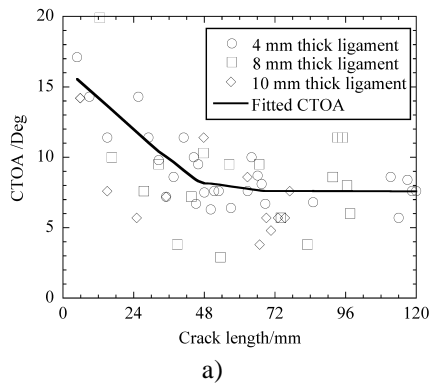

a)   b)

Figure 4: showing a) CTOA as a function of crack growth and b) 8mm thick shear specimen after the test.

the best-fitted values of GT parameters. The experimental CTOA was estimated directly from the captured video images. Figures 3a-d show some of these. The strong levels of plastic deformation around the moving crack tip deflect the ligament surface from flat, which makes the precise CTOA measurement quite complicated. Figure 4a shows the measured CTOA values for three specimen thicknesses. The steady state CTOA values, corresponding to established slant crack growth, were achieved after the crack had grown 5-12 thicknesses. The value for $CTOA_C$ was found to be about 8°. This result correlates with that reported by Dawicke et al [17-19] for aircraft aluminium. However the steady state for aluminium was
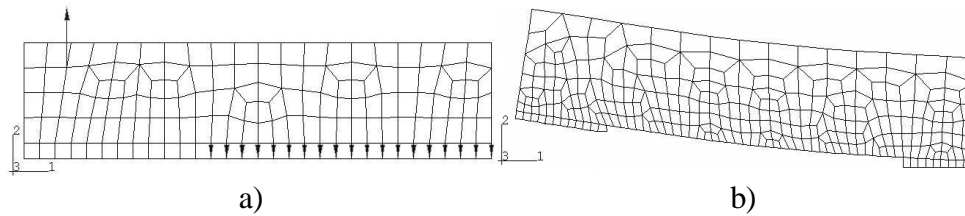
a)   b)

Figure 5: showing a) initial and deformed meshes of half of an 8-mm thick ligament shear specimen.

achieved after about 2-3 thicknesses.

This $CTOA_C$ value was used in FE modelling of the shear test as the criterion for the best-fitted GT parameters. A simplified 2D mesh representing only one half of the specimen was used. The damage cell sizes were chosen according to [20] as 3.36 mm for 4mm thick specimens, 6.67 mm for 8mm thick specimens and 8.35 mm for 10mm thick specimens. These values depend on the specimen geometry, primarily thickness. Initial and deformed meshes for the 8mm thick specimen are shown in Figure 5, where the extensive crack growth is seen.

The best-fitted GT parameters were found as $q_1 = 1.6$, $q_2 = 1.5$, $q_3 = 2.56$. Thus there is a marked difference in q_2 values between the flat and slant fractures. This is consistent with the hypothesis that q_2 is a function of the triaxiality of the component stress state.

CHARPY TEST MODELLING

Charpy tests on TL-oriented specimens were carried out and the values of total energy absorbed values were obtained in the range 200-220 J. One of the broken Charpy samples in shown in Figure 1c.

Symmetry conditions allowed the use of a mesh of only one quarter of the full specimen. Material with ductile properties (with GT parameters tuned on modelling of the shear test) was used in layers of FE on the side surface of the mesh. The layers of elements situated close to the vertical symmetry plane were used to simulate the flat fracture, so that GT parameters, tuned on modelling of notch tensile specimens were used for these elements.

It was found that the Charpy energy obtained via FE modelling depends on the amount of FE layers with shear (or flat) properties. This is shown in Figure 6. The best correspondence with the experimental energy values was
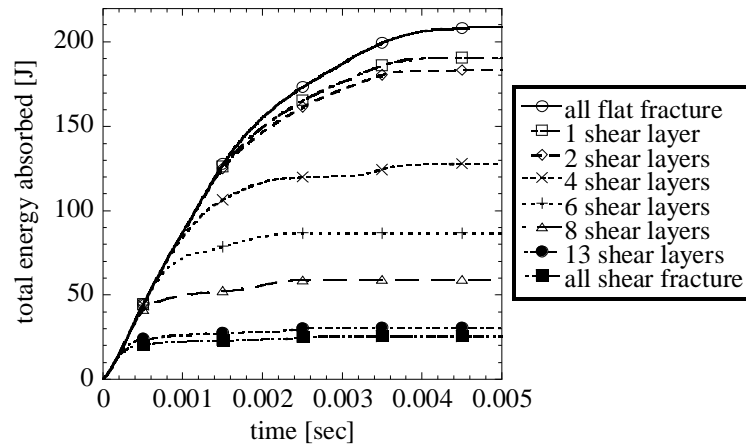
Figure 6: Charpy energy – time curves for different amounts of shear layers obtained via FE modelling.

obtained with the model containing two layers of elements with shear properties and the rest with flat fracture properties. This result correlates qualitatively with what is observed in practice. However the present analysis does not take into account the existence of delaminations (Figure 1c).

CONCLUSIONS

The techniques of ductile damage mechanics were used to cross-correlate the experimental information obtained from notch tensile (load – diametral contraction), special shear (CTOA) and conventional Charpy (total energy absorbed) tests. The effect of the amount of shear fracture on the Charpy energy was shown.

REFERENCES

1. Killmore, C.R., Barbaro, F.J., Williams, J.G. and Rothwell, A.B. (1997). In: *Fracture Control in Gas Pipelines*, pp. 4-1 – 4-19, Cutler, J. (Ed.). WTIA/APIA/CRC-MWJ, Sydney.
2. Jones, R., Rothwell, A.B. (1997). In: *Fracture Control in Gas Pipelines*, pp. 5-1 – 5-21, Cutler, J. (Ed.). WTIA/APIA/CRC-MWJ, Sydney.
3. Europipe. (1996) Test certificate 3.1B – EN 10204, Order: 645/3168, Item: 001, Certificate: 96-0155, Section: 1.

4. Gurson, A.L. (1977) *Journal of Engineering Materials and Technology* **99**, 2.

5. Tvergaard, V. (1981) *International Journal of Fracture Mechanics* **17**, 389.

6. Needleman, A. and Tvergaard, V. (1987) *Journal of the Mechanics and Physics of Solids* **35**, 151.

7. Franklin, A.G. (1969) *Journal of Iron and Steel Institute* **207**, 181.

8. Burstow, M.C., Howard, I.C., Pugh, A.C., Yates, J.R. and Swan, D.I. (2000). In: *Applications of fracture mechanics in failure assessment, PVP-Vol. 412*, pp. 53-61, Lidbury, D. (Ed.). ASME.

9. Burstow, M.C., Howard, I.C., Pugh, A.C. and Yates, J.R. (1999). Departmental report SIRIUS-DDG-99-5, Department of Mechanical Engineering, The University of Sheffield.

10. Burstow, M.C., Howard, I.C. (1996) *Fatigue and Fracture of Engineering Materials and Structures* **19**, 461.

11. Burstow, M.C., Howard, I.C. and Ainsworth, R.A. (1998) *International Journal of Fracture* **89**, 117.

12. Baczynski, G.J., Jonas, J.J. and Collins, L.E. (1999) *Metallurgical and Material Transactions* A **30**, 3045.

13. Miglin, M.T., Hirth, J.P. and Rosenfield, A.R. (1983) *International Journal of Fracture* **22**, R65.

14. Rivalin, F., Pineau, A., Di Fant M. and Besson J. (2001) *Engineering Fracture Mechanics* **68**, 329.

15. Pussegoda, N., Malik, L., Dinovitzer, A., Graville, B.A. and Rothwell, A.B. (2000) In: *Pipeline technology*, pp. 239-245, Denys, R. (Ed.). Elsevier, Netherlands.

16. Pussegoda, N., Verbit, S., Dinovitzer, A., Tyson, W., Glover, A., Collins, L., Carlson, L. and Beattie, J. (2000) In: *Pipeline technology*, pp. 247-254, Denys, R. (Ed.). Elsevier, Netherlands.

17. Dawicke, D.S., Sutton, M.A. (1994) *Experimantal Mecanics* **34**, 357.

18. Dawicke, D.S., Piascik, R.S. and Newman, J.C. Jr. (1997) In: *Fatigue and fracture mechanics, ASTM STP 1321*, pp. 309-24, Underwood, J.H., Macdonald, B.D. and Mitchell, M.R. (Eds.). ASTM.

19. Dawicke, D.S., Newman, J.C. Jr. and Bigelow, C.A. (1995) In: *Fracture mechanics, ASTM STP 1256*, Reuter, W.G., Underwood, J.H. and Newman, J.C. Jr. (Eds.). ASTM.

20. O'Donohue, P.E., Kanninen, M.F., Leung, C.P., Demofonti, G. And Venzi, S. (1997) *International Journal of Pressure Vessels and Piping* **70**, 11.